Dalton Transactions

Accepted Manuscript

ROYAL SOCIETY OF CHEMISTRY

www.rsc.org/dalton

Cite this: DOI: 10.1039/c0xx00000x

www.rsc.org/xxxxxx

ARTICLE TYPE

Tris(hydroxymethyl)aminomethane Modified Layered Double Hydroxides Largely Facilitate Polyoxometalate Intercalation

Yang Chen,[†] Dongpeng Yan,[†] and Yu-Fei Song*

Received (in XXX, XXX) Xth XXXXXXXXX 20XX, Accepted Xth XXXXXXXXX 20XX

DOI: 10.1039/b000000x

Polyoxometalates (POMs) intercalation to layered double hydroxides (LDHs) has been greatly restricted by the geometry, charge and size of POMs. We report herein, for the first time, the intercalation of $Na_3[PW_{12}O_{40}]\cdot 15H_2O$ into tris(hydroxymethyl)-aminomethane (Tris) modified layered double hydroxides (Tris-LDH-CO_3) using ion exchange method, resulting in the formation of novel intercalated Tris-LDH-PW_{12} under ambient conditions without necessity of degassing CO_2. Theoretical calculations show the decreased energy and the slightly distorted LDH layer after Tris modification, indicating the Tris-modified LDHs layer largely facilitate the intercalation of PW_{12}. Further application of Tris-LDH-PW_{12} for oxygenation of sulfides shows highly efficient and selective catalytic activities under mild condition. The Tris-LDH-PW_{12} can be easily recovered and reused for more than 10 times without obvious decrease of reactivity. This opens a completely new pathway for engineering POMs-LDHs advanced functional materials.

Introduction

Polyoxometalates (POMs) are a class of discrete anionic metal-oxide clusters with unrivalled structural types[1, 2] as well as a wide range of unique physical properties and applications in areas as diverse as catalysis,[3, 4] medicine[5] and nano-science.[6] Layered double hydroxides (LDHs) comprise an unusual class of layered materials with positively charged nanosheets/layers and the balancing anions located in the interlayer region.[7-10] The POMs/LDHs nanocomposites have attracted wide interests as they have shown great advantages over both traditional LDHs and POMs compounds.[11-15] Although POMs intercalated LDHs possess superior application than POMs or LDHs, the relevant intercalation process faces serious challenges: 1) It is almost impossible to obtain POMs/LDHs nanocomposites with no impurity using traditional synthetic methods such as co-precipitation and reconstitution pathways *etc*; 2) The POMs intercalation is closely related to the geometry, charge and size of POMs.[12] As such, a number of POMs anions such as the classical Keggin cluster of $[PW_{12}O_{40}]^{3-}$ with the negative charge below 4 are very unlikely to intercalate into LDHs using the conventional synthetic methods; 3) LDHs exhibit high affinity for CO_3^{2-} anions, and ion exchange reactions for preparation of POMs intercalated into LDHs do not work in air in most cases.[16]

Since the strong affinity between POMs layers and guest CO_3^{2-} anions originates from the electrostatic interactions and hydrogen bonding, it is highly interesting whether it is possible to decrease such host-guest interactions, and thereby promote the ion exchange. Bearing this in mind, and inspired by recent work on the tris(hydroxymethyl)aminomethane (Tris) modified LDHs (Tris-LDH-CO_3),[17] we report, for the first time, ion exchange of the Tris-LDH-CO_3 with classical Keggin cluster of $Na_3PW_{12}O_{40}\cdot 15H_2O$ (Na-PW_{12}) under ambient conditions without the necessity of degassing CO_2 (Scheme 1). As a result, Tris-LDH-PW_{12} can be prepared for the first time using ion exchange method.

Scheme 1 Schematic representation of the synthesis of $[PW_{12}O_{40}]^{3-}$ intercalated into Tris-stabilized LDHs.

Experimental Section

Chemicals: All the used chemicals and solvents were purchased from Alfa Aesar and used directly without further purification.

Characterization: Powder X-ray diffraction (XRD) patterns were recorded on a Rigaku XRD-6000 diffractometer under the following conditions: 40 kV, 30 mA, Cu Kα radiation (λ = 0.154

nm). FT-IR spectra were recorded on a Bruker Vector 22 infrared spectrometer by using KBr pellets. The solid state NMR experiments were carried out at 75.6 MHz for ^{13}C and 121.0 MHz for ^{31}P on a Bruker Avance 300M solid-state spectrometer equipped with a commercial 5 mm MAS NMR probe. The N_2 adsorption-desorption isotherms were measured using Quantachrome Autosorb-1 system at liquid nitrogen temperature. Scanning electron microscopy (SEM) images and energy dispersive X-ray (EDX) analytical data were obtained using a Zeiss Supra 55 SEM equipped with an EDX detector. Transmission electron microscopy (TEM) micrographs were recorded using a Hitachi H-800 instrument. HRTEM images were conducted on a JEOL JEM-2010 electron microscope operating at 200 kV. Thermogravimetric and differential thermal analyses (TG-DTA) were performed on a TGA/DSC 1/1100 SF from Mettler Toledo in flowing N_2 with a heating rate of 10 $^oC \cdot min^{-1}$ from 25 ^oC to 1000^oC. X-ray photoelectron spectroscopy (XPS) measurements were performed with monochromatized Al Kα exciting X-radiation (PHI Quantera SXM). Inductively coupled plasma emission spectroscopy (ICP-ES, Shimadzu ICPS-7500) was used to measure the concentration of W in the catalysts. GC analyses were performed with Agilent 7820A GC system by using a 30 m 5% phenymethyl silicone capillary column with an ID of 0.32 mm and 0.25 mm coating (HP-5).

Desulfurization experiments: In a typical experiment, a solution of dibenzothiophene (DBT), benzothiophene (BT), and 4,6-dimethyl-dibenzothiophene (4,6-DMDBT) in n-octane was used as model oil with an S content of 1000 ppm. The catalytic oxidative desulfurization experiments were performed in a 50 mL two-necked flask, to which 0.08 mL of 30 wt% H_2O_2, 5 mL of model oil, 1 mL of [bmim]BF_4, and Tris-LDH-PW_{12} (H_2O_2/DBT/Cat = 100:20:1) were added. The reaction mixture was stirred at 75 ^oC. During the reaction, the upper layer of the model-oil phase was periodically withdrawn and analyzed by gas chromatography with a flame ionization detector (GC-FID). DBT, BT, and 4,6-DMDBT were identified by using reference standards.

Oxygenation of sulfides: 1 mmol substrate, 30% H_2O_2 aqueous solution, 0.25mol% catalyst (Tris-LDH-PW_{12} contain polyoxometalate anions 2.5μmol) and 0.2 ml n-propanol were placed in a 20 ml glass bottle at room temperature and the reaction mixture was kept stirring vigorously. The reaction was effectively quenched after 5 h. The resulting oily products were extracted with diethyl ether, analyzed by gas chromatography with a flame ionization detector (GC-FID). The conditions were as follows: injection port temperature 340 ^oC; detector temperature250 ^oC; oven temperature 70 ^oC; carrier gas: ultrapure nitrogen; sample injection volume 1 mL.

Preparation: $Na_3[PW_{12}O_{40}]\cdot 15H_2O$[18] (Na-$PW_{12}$) and the tripodal ligand-stabilized layered double hydroxide (Tris-LDH-CO_3)[17] were synthesized according to the literature procedures, respectively. The POMs were intercalated into Tris-LDH-CO_3 by using anion-exchange method under CO_2-existing conditions. Tris-LDH-CO_3 (2 mg/mL) was re-dispersed in the $Na_3[PW_{12}O_{40}]$ solution (0.1 M) then stirred 2 h at room temperature. The precipitate was then filtered, washed with water and acetone, and dried in an oven to obtain the Tris-LDH-PW_{12}.

Results and Discussion

Synthesis and Characterization of Tris-LDH-PW_{12}

Tris-modified layered double hydroxides (LDHs) has been prepared successfully by mixing $MgCl_2$, $AlCl_3$ and Tris in aqueous solution, leading to the formation of Tris-LDH-CO_3.[17] Ion exchange of the classical Na-PW_{12} with Tris-LDH-CO_3 under ambient conditions without necessity of degassing CO_2 results in the formation of new intercalated assembly of Tris-LDH-PW_{12}. The XRD patterns of the Tris-LDH-CO_3 (Figure 1) show the characteristic (003), (006), (110) and (113) at 2θ = 11.5°, 23.4°, 60.9° and 62.2°. After ions exchange of CO_3^{2-} with $[PW_{12}O_{40}]^{3-}$, the XRD patterns of Tris-LDH-PW_{12} show the (003) and (006) at 2θ = 8.4° and 18.1°, corresponding to d values of 1.1 and 0.5 nm, respectively. Compared with the XRD pattern of Tris-LDH-CO_3, the basal (003) and (006) reflections of Tris-LDH-PW_{12} shift to lower 2θ, indicating the successful intercalation of $[PW_{12}O_{40}]^{3-}$ into the Tris-modified layer double hydroxides. It is noted that 1.1 nm ≈ 2 ×0.5 nm, which suggests a typical layered structure of Tris-LDH-PW_{12}.[19] Based on the elemental analysis [Mg = 4.13%, Al = 2.29%, W = 62.53% and N = 0.35%], elemental composition of the product can be expressed as $Mg_{0.66}Al_{0.33}(C_4H_8NO_3)_{0.097}(OH)_{1.71}(PW_{12}O_{40})_{0.11}\cdot 0.68H_2O$ (Table S1).

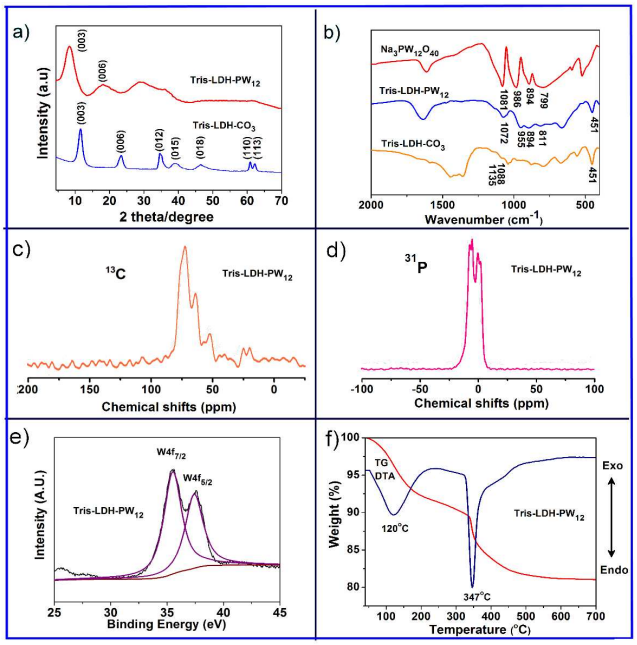

Fig. 1 a) The XRD patterns of the Tris-LDH-CO_3 and Tris-LDH-PW_{12}; b) FT-IR spectra of Tris-LDH-CO_3, Tris-LDH-PW_{12} and $Na_3PW_{12}O_{40}$; c) ^{13}C and d) ^{31}P CP/MAS NMR spectra of Tris-LDH-PW_{12}; e) XPS spectra for the W4f core level spectrum of the Tris-LDH-PW_{12}; f) TG−DTA of Tris-LDH-PW_{12}.

As Pinnavaia *et al* pointed out that it is very unlikely to intercalate the classical Keggin cluster of $[PW_{12}O_{40}]^{3-}$ into the LDHs because of its negative charge below 4.[12] In contrast, the mono-lacunary Keggin cluster of $[PW_{11}O_{39}]^{7-}$ (PW_{11}) has been intercalated into LDHs as contrast (Figure S1). The resulting LDH-PW_{11} exhibits the reflections of the layered structure with

(003) and (006) at 2θ = 6.1° and 12.1°, corresponding to *d* values of 1.5, and 0.7 nm, respectively. Moreover, a broad diffraction following (003) can be observed, which is rather common in various POM-intercalated LDH materials using the conventional synthetic methods[20]. Therefore, the Tris-modified layer double hydroxides show much improved intercalation ability in comparison to that of classical LDHs. Moreover, no impurity can be observed in the XRD patterns of Tris-LDH-PW_{12}, which is in good contrast to those of the conventional POMs intercalated LDHs.

FT-IR spectra of Tris-LDH-CO_3, Tris-LDH-PW_{12} and $NaPW_{12}O_{40}$ are shown in Figure 1b. The absorption bands at 1088 and 1135 cm^{-1} in the spectrum of Tris-LDH-CO_3 are due to the characteristic stretching vibration of M−O−C and C−C−O, respectively.[17] . The asymmetric vibration peak 1072 cm^{-1} for P−O chemical bond still exists in the Tris-LDH-PW_{12}. The asymmetric vibration of W−O bond also changes significantly and the shift is from 986 cm^{-1} in $Na_3PW_{12}O_{40}$ to 955 cm^{-1}, the characteristic absorption bands shift to lower frequency indicates the presence of strong electrostatic interactions and hydrogen bondings between the host layers and the guest anions.[21] The peaks at 894 and 811 cm^{-1} in Tris-LDH-PW_{12} are assigned to the vibration of W−O−W chemical bonds, which are originally at 894 and 799 cm^{-1}, respectively. These results reveal that $[PW_{12}O_{40}]^{3-}$ anions still hold the Keggin structure upon intercalation. The absorption band in the range of 400−800 cm^{-1} in Tris-LDH-CO_3 or Tris-LDH-PW_{12} can be ascribed to O−M−O vibrations in the brucite-like layers of LDH.[22]

The ^{13}C CP/MAS NMR spectrum of Tris-LDH-CO_3 (Figure S2) shows a strong signal at 171 ppm, which can be assigned to the interlayer CO_3^{2-} species.[17] In the case of Tris-LDH-PW_{12}, no signal at ~170 ppm can be observed (Figure 1c), which is due to the successful exchange of $[PW_{12}O_{40}]^{3-}$ with the inter-layered CO_3^{2-}. One set of signals centred at δ = -4 ppm for the $[PW_{12}O_{40}]^{3-}$ anions in the ^{31}P NMR spectrum of Tris-LDH-PW_{12} (Figure 1d), suggesting the $[PW_{12}O_{40}]^{3-}$ anions have been intercalated into the Tris-modified LDHs. The energy-dispersive X-ray (EDX) result of Tris-LDH-PW_{12} (Figure S3) reveals the presence of Mg, Al, C, N, P and W elements, and the P/W molar ratio close to the expected 12/1, indicating the completeness of $[PW_{12}O_{40}]^{3-}$ anions in the interlayer of Tris-modified LDHs.

XPS analysis has been employed to characterize the oxidation state of W species in the Tris-LDH-PW_{12} (Figure 1e). The XPS curve fitting procedure is according to the theory of Doniach and Sunjic.[23] The W4f spectrum can be deconvoluted into doublets, as indicated in Figure 1e. This doublet consists of $W4f_{7/2}$ line at 35.5 eV and $W4f_{5/2}$ at 37.5 eV, which are assigned to the W in the W-O bond configuration and typically observed for the W^{6+}.[24] All of these results reveal that the Keggin structure is retained after being intercalated into Tris-modified LDHs. This has been further proved by the theoretical calculation below.

Thermogravimetry (TG) and differential thermal analysis (DTA) curves for Tris-LDH-PW_{12} are shown in Figure 1f. Two weight-loss stages can be observed with the increase of temperature from 75 to 700 °C. The first weight loss of 8.39% at 75−220 °C corresponds to the loss of surface and interlayer adsorbed water. The second weight loss step of 10.49% at 220−660 °C can be attributed to the decomposition of the Tris on LDHs and the collapse of the layered structure. Two endothermic peaks in the DTA curve can be observed at 120 °C and 347 °C.

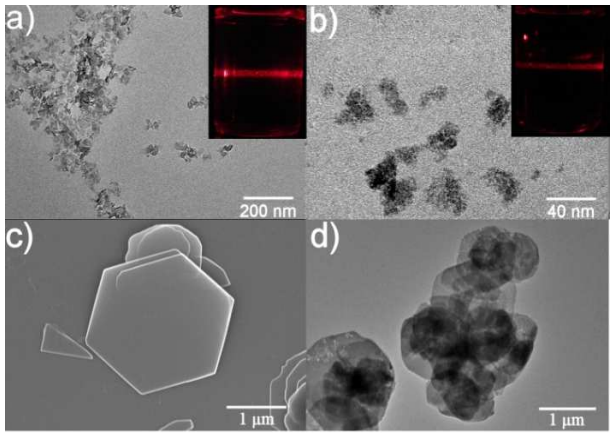

Fig. 2 (a) TEM image and the corresponding Tyndall effects (inset) of Tris-LDH-CO_3, (b) HRTEM image and the corresponding Tyndall effects (inset) of Tris-LDH-PW_{12}; SEM images of the conventional LDH: (c) LDH-CO_3 and (d) LDH-PW_{11}.

TEM image (Figure 2a) of Tris-LDH-CO_3 shows the uniform nanoparticles with a rectangular shape and average size ~20 nm, which is very different from the conventional LDH-CO_3 with the plate shape and the average size of several hundreds nanometre (Figure 2c). HRTEM image of Tris-LDH-PW_{12} exhibits irregular morphology with uniform dispersion of $[PW_{12}O_{40}]^{3-}$ as small black dots (Figure 2b). In contrast, the hexagonal plate morphology of LDH-PW_{11} can be clearly observed in the TEM images (Figure 2d). The colloidal dispersions of Tris-LDH-CO_3, Tris-LDH-PW_{12} are transparent and show the typical Tyndall effect (Inset in Figure 2a and 2b), indicating the presence of highly dispersed colloidal solution.

Table 1 Comparison of physio-chemical properties of Tris-LDH-CO_3 and Tris-LDH-PW_{12}

Materials	Surface area (m^2/g)	Pore volume (cm^3/g)	Average pore diameter (nm)
Tris-LDH-CO_3	58.8	0.096	4.2
Tris-LDH-PW_{12}	15.9	0.018	3.8

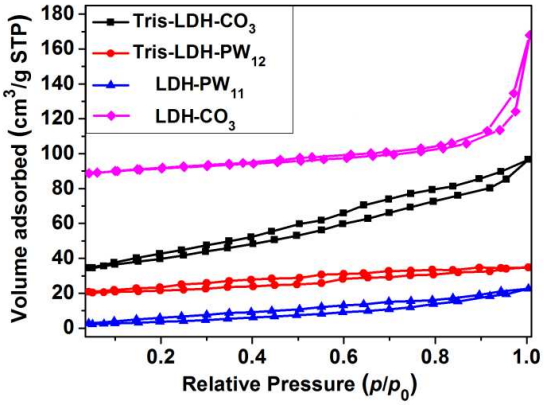

Fig. 3 Adsorption–desorption isotherms of Tris-LDH-CO_3, Tris-LDH-PW_{12} and the conventional LDH including LDH-CO_3, LDH-PW_{11}.

BET measurements have been carried out on the Tris-LDH-CO_3 and Tris-LDH-PW_{12}. The specific surface area, pore volume,

and average pore diameter (estimated from N_2 adsorption–desorption isotherms) are presented in Table 1. BET data shows that the surface area of Tris-LDH-CO_3 and Tris-LDH-PW_{12} of 58.8 and 15.9 m^2/g, pore volume of 0.096 and 0.018 cm^3/g, average pore diameter of 4.2 and 3.8 nm, respectively. Furthermore, Tris-LDH-CO_3 and Tris-LDH-PW_{12} display H4 type hysteresis loops (Figure 3), indicating that the pores are produced by the aggregation of slit-shaped pores with some microporosity,[25] which is similar to the conventional Mg_3Al-PW_{11}, but different from the conventional Mg_3Al-CO_3 with H3 type hysteresis loops.[26] It is worthwhile noting that despite the surface area and pore volume of Tris-LDH-PW_{12} are smaller than that of Tris-LDH-CO_3, the nanoscale particles of Tris-LDH-PW_{12} guarantee the well-dispersion and thereby facilitate the access of the substrates to the active species. As such, Tris-LDH-PW_{12} shows excellent catalytic activity.

Theoretical Calculations

To further understand how the Tris-modified LDHs can tailor the host-guest interactions within the interlayer region, periodic density functional theoretical (DFT) calculations have been employed for the idealized models of LDH-CO_3, LDH-PW_{12}, Tris-LDH-CO_3 and Tris-LDH-PW_{12} structures (Figure S4). The typical optimized structures for LDHs before and after Tris-modification are shown in Figure 4.

It can be observed that the Tris units can accommodate at both the inner and outer of the LDH layers, which do not affect the change in the basal spacing relative to the pristine form. This is consistent with the fact that the modification by Tris has the same possibility at two sides of the LDH layers. Upon the increasing the Tris units anchored on the LDH layer, the values of lattice energy for both LDH-CO_3 and LDH-PW_{12} have a decreasing trend (ca. 247 hartree per Tris unit, Table S2), which shows that the LDH lattice can be highly stabilized upon formation of the Tris-modified LDHs structures. The decreased energy and observed slightly distorted LDH layer after surface modification by Tris further suggest that the flexible Tris-modified LDHs layer may facilitate the intercalation of PW_{12} as observed in the experiment. Moreover, the configuration of the PW_{12} anions is nearly unchanged upon intercalation, which is in agreement well with the FT-IR and XPS results.

In addition, to detect the influences of the different models on the calculation results, a 4×3×1 Mg-Al-LDH supercell (Figure S5, denoted as **Model 2**) has been further selected to accommodate the pure PW_{12} anions in the absence of intercalated CO_3^{2-}. It can be observed that the calculated lattice energy for the LDH-PW_{12} shows a similar decreasing trend (Table S3) upon increasing the Tris units as those of the calculation with the 6×4×1 LDH layer in the presence of intercalated CO_3^{2-}. Moreover, it is also observed that the electron density of the HOMOs and the LUMOs are mainly populated on the W and O atoms of the interlayer PW_{12} (Figure S6). These results confirm that the selected models (such as different sizes of the LDH layer and in the presence/absence of the co-intercalated CO_3^{2-}) do not influence the calculation conclusions obviously.

Electronic densities of states (DOS) and frontier orbital analysis (Figure S7-S8) show that for the LDH-PW_{12} system, the electron density of the highest occupied molecular orbitals (HOMOs) and the lowest unoccupied molecular orbitals (LUMOs) are mainly contributed from W and O atoms of the PW_{12} anions, and the LDH layer do not participate in the frontier orbital distribution (Figure S9). These suggest that there is no electronic transfer occurs between the LDH and PW_{12}, and the valence electrons localized in the PW_{12} are confined within the energy blocking by the LDH layers. Similar results were also obtained for the Tris-LDH-PW_{12} system (Figure S10-S12), suggesting that there is no obvious change in the energy levels and active sites of the Tris-LDH-PW_{12} system after the Tris modification. This conclusion is also in agreement with the XPS observation above.

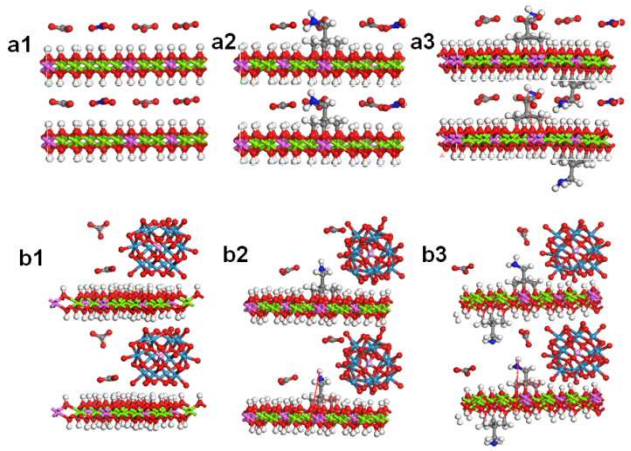

Fig. 4 The optimized geometric structures of the a1) LDH-CO_3; a2) and a3) Tris-LDH-CO_3; b1) LDH-PW_{12}; b2) and b3) Tris-LDH-PW_{12}.

Application of Tris-LDH-PW_{12} for oxygenation

To further explore the potential application of Tris-LDH-PW_{12}, it has been applied for extraction and catalytic desulfurization (ECODS) of dibenzothiophene (DBT), experiments have been carried out with H_2O_2/DBT/Cat = 100:20:1 at 75°C. The percentage sulfur removal and C_t are plotted against reaction time in Figure 5a, in which C_0 and C_t are the initial DBT concentration and DBT concentration at time t, respectively. The linear fit of the data reveals that the catalytic reaction exhibits zero-order kinetics for the desulfurization process with $R^2 = 0.9953$. The rate constant k of the oxidation reaction was determined to be 41.5 $mgL^{-1}min^{-1}$ on the basis of Equations (1) and (2). The oxidation of DBT to $DBTO_2$ can be completed in about 25 min. As such, the catalyst shows high catalytic efficiency for the oxidation of sulfide to sulfone, and the catalytic reaction strictly obeys zero-order kinetics with almost 100% selectivity for $DBTO_2$.

$$-\frac{dC_t}{dt} = k \quad (1)$$

$$C_0 - C_t = kt \quad (2)$$

In the case of 4,6-dimethyldibenzothiophene (4,6-DMDBT) and benzothiophene (BT), which are difficult to remove owing to the relatively lower electron density of sulfur atoms on both substrates,[27] the catalytic system exhibits a high desulfurization efficiency with almost 100% sulfur removal for 4,6-DMDBT and BT in 55 and 60 min, respectively (Figure 5b).

Table 2. Comparison of catalytic oxidative desulfurization of DBTs by using different catalysts containing $[PW_{12}O_{40}]^{3-}$ or LDH reported in the literature and Tris-LDH-PW_{12}.

Entry	Catalysts	oxidant	T [°C]	t [min]	S [ppm]	S removal [%]	Ref.
1	$[(C_{18}H_{37})_2N(CH_3)_2][PW_{12}O_{40}]$	H_2O_2	60	40	500	96	28
2	$Na_2HPW_{12}O_{40}$	H_2O_2	60	150	5700	95	29
3	$H_3PW_{12}O_{40}$	H_2O_2	60	60	500	99	30
4	SBA15-PW_{12}	*t*-BuOOH	70	120	174	97	31
5	$[MIMPS]_3PW_{12}O_{40}\cdot 2H_2O$	H_2O_2	30	60	500	100	32
6	LDH-WO_4	H_2O_2	70	60	18400	29	33
7	LDH-WO_4	H_2O_2	40	180	18400	90	34
8	Tris-LDH-PW_{12}	H_2O_2	75	25	1000	99	this work

Note: SBA15-PW_{12} = SBA15-$H_3PW_{12}O_{40}$, MIMPS = 1-(3-sulfonic group) propyl-3-methyl imidazolium phosphotungstate.

To compare the catalytic oxidative desulfurization efficiency of Tris-LDH-PW_{12} with $[PW_{12}O_{40}]^{3-}$ or LDH-containing catalysts reported in the literature, we have summarized the results in Table 2. It can be seen that deep desulfurization of DBT can be achieved by using Tris-LDH-PW_{12} in 25 min at 75 °C with H_2O_2/DBT/Cat = 100:20:1 (Table 2, entry 8), which is one of the highly efficient catalysts reported so far. The main advantage of heterogeneous catalysts in a liquid-phase reaction is the ease of separation and reuse of the catalyst in catalytic cycles. As such, the recycled Tris-LDH-PW_{12} catalyst has been applied for further oxidation of DBT. After the desulfurization procedure, the upper layer can be separated by decantation. Then, 50 mL of deionized water is added to the water phase to decrease the viscosity of $[bmim]BF_4$. After that, the catalyst can be separated by centrifugation and filtration. The diluted $[bmim]BF_4$ in deionized water is concentrated under vacuum to recycle the ionic liquid. As such, the IL and catalyst are both reusable. The catalyst can be recycled and reused at least ten times without obvious decrease of the catalytic efficiency (Figure 5c). The recycled catalyst and the oxidative product have been characterized (Figure S13-S15).

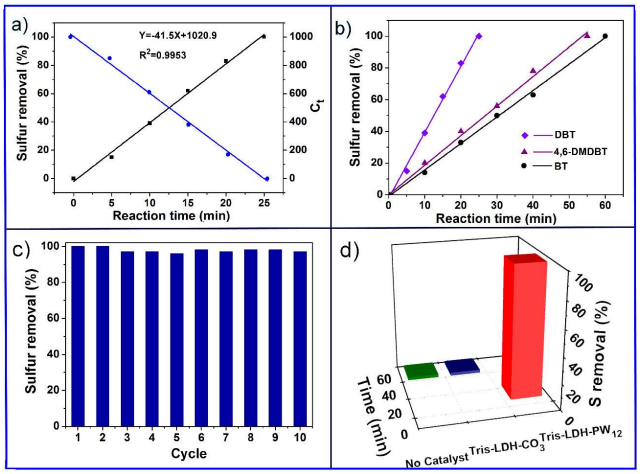

Fig. 5 a) Sulfur removal of DBT; C_t as a function of reaction time at 75°C; b) The comparison of the reactivity of DBT, 4,6-DMDBT, BT; c) The recycling experiments for desulfurization of DBT using Tris-LDH-PW_{12} at 75°C; d) Comparison of sulfur removal efficiency of different catalytic systems. Reaction conditions: T = 75°C, H_2O_2 = 0.080 mL, model oil = 5 mL (S = 1000 ppm), $[bmim]BF_4$ = 1 mL, H_2O_2/DBT/Cat = 100:20:1.

Comparative experiments using Tris-LDH-CO_3/H_2O_2/$[bmim]BF_4$ and/or H_2O_2/$[bmim]BF_4$ as desulfurization systems (Figure 5d) show sulfur removal efficiency is less than 20% in 60 min, whereas the Tris-LDH-PW_{12}/H_2O_2/$[bmim]BF_4$ exhibits 99% desulfurization in only 25 min by applying the experimental conditions of T = 75 °C, H_2O_2 = 0.080 mL, model oil = 5 mL (S = 1000 ppm), $[bmim]BF_4$ = 1 mL, H_2O_2/DBT/Cat = 100:20:1. This result indicates the synergetic interactions between the Tris-modified LDHs and the intercalated PW_{12} anions lead to the large enhancement of the desulfurization efficiency in the presence of H_2O_2 and $[bmim]BF_4$. Besides used for extraction and catalytic oxidative desulfurization (ECODS), Tris-LDH-PW_{12} can also be applied for oxidation of various sulfides. As shown in Table 3, different sulfides are oxygenated to the corresponding sulfones (ca. 100%) with >99% selectivity. These experiments suggest that sulfides could be effectively oxidized by Tris-LDH-PW_{12}.

Table 3. Oxygenation of sulfides by the Tris-LDH-PW_{12} in the presence of H_2O_2.[a]

Entry	substrate	(sulfoxide% /sulfone%)	Yield (%)
1	methyl p-tolyl sulfide	(0/100)	100
2	allyl phenyl sulphide	(0/100)	100
3	tetrahydrothiapyran	(0/100)	100
4	4-chlorothioanisole	(0/100)	100
5	ethyl phenyl sulfide	(0/100)	100
6	thioanisole	(0/100)	100
7	diethyl sulfide	(0/100)	100
8	4-nitrophenylsulphide	(0/100)	100
9	4-methoxythioanisole	(0/100)	100
10	4-bromothioanisole	(0/100)	100

a Reaction conditions: Sulfide 1 mmol, Tris-LDH-PW_{12} 2.5 µmol, H_2O_2 (30% aq.) 3 mmol, 1-Propanol 200 µl , 25°C, 5h. Conversion and selectivity were determined by GC.

Conclusions

In summary, we have prepared for the first time $Na_3[PW_{12}O_{40}]$ intercalated Tris-modified LDHs without necessity of degassing CO_2, which results in the formation of new intercalated assembly of Tris-LDH-PW_{12} under mild conditions. This can't be realized using the traditional synthetic methods due to the limitation of the $[PW_{12}O_{40}]^{3-}$ charge below 4. The XRD patters of Tris-LDH-PW_{12} indicate clearly that no impurity phase after (003) diffraction, which is in good contrast to the conventional POMs intercalated LDHs materials. Further application of Tris-LDH-PW_{12} for oxygenation of sulfides with 30% H_2O_2 exhibits highly efficient catalytic results under mild conditions. The nanoscale particles of

Tris-LDHs-PW_{12} promote the well-dispersion of the catalysts and the access of the active species to the substrates. As such, Tris-modified LDHs change the host-guest interactions, and thereby largely facilitate PW_{12} intercalation. Most importantly, it opens a completely new pathway for the development of POMs-LDHs advanced functional materials.

Acknowledgements

This research was supported by the National Basic Research Program of China (973 program, 2014CB932104), National Science Foundation of China (21222104), and Fundamental Research Funds for the Central Universities (RC1302) and the Program for Changjiang Scholars and Innovative Research Team in University.

Notes and references

State Key Laboratory of Chemical Resource Engineering
Beijing University of Chemical Technology
Beijing 100029, P. R. China
E-mail: songyufei@hotmail.com *or songyf@mail.buct.edu.cn*
† These authors have the same contribution.

‡Electronic Supplementary Information (ESI) available: Sample characterization, Calculation details and analysis of Tris-LDH-CO_3 and Tris-LDH-PW_{12}. See DOI: 10.1039/b000000x/

1. D.-L. Long, E. Burkholder and L. Cronin, *Chem. Soc. Rev.*, 2007, **36**, 105-121.
2. A. Müller, P. Kögerler and A. W. M. Dress, *Coord. Chem. Rev.*, 2001, **222**, 193-218.
3. M. V. Vasylyev and R. Neumann, *J. Am. Chem. Soc.*, 2003, **126**, 884-890.
4. N. Mizuno, K. Yamaguchi and K. Kamata, *Coord. Chem. Rev.*, 2005, **249**, 1944-1956.
5. B. Hasenknopf, *Front. Biosci*, 2005, **10**, 275-287.
6. C. Fleming, D.-L. Long, N. McMillan, J. Johnston, N. Bovet, V. Dhanak, N. Gadegaard, P. Kögerler, L. Cronin and M. Kadodwala, *Nat. Nanotech.*, 2008, **3**, 289-233.
7. Q. Wang and D. O'Hare, *Chem. Rev.*, 2012, **112**, 4124-4155.
8. A. Fogg, V. Green, H. Harvey and D. O'Hare, *Adv. Mater.*, 1999, **11**, 1466-1469.
9. W. Shi, S. He, M. Wei, D. G. Evans and X. Duan, *Adv. Funct. Mater.*, 2010, **20**, 3856-3863.
10. M. Q. Zhao, Q. Zhang, X. L. Jia, J. Q. Huang, Y. H. Zhang and F. Wei, *Adv. Funct. Mater.*, 2010, **20**, 677-685.
11. E. D. Dimotakis and T. J. Pinnavaia, *Inorg. Chem.*, 1990, **29**, 2393-2394.
12. T. Kwon and T. J. Pinnavaia, *J. Mol. Catal.*, 1992, **74**, 23-33.
13. S. K. Yun, V. R. L. Constantino and T. J. Pinnavaia, *Microporous Mater.*, 1995, **4**, 21-29.
14. J. Evans, M. Pillinger and J. Zhang, *J. Chem. Soc., Dalton Trans.*, 1996, 2963-2974.
15. S. Zhao, J. Xu, M. Wei and Y.-F. Song, *Green Chem.*, 2011, **13**, 384-389.
16. F. Kooli, C. Depege, A. Ennaqadi, A. De Roy and J. Besse, *Clays Clay Miner.*, 1997, **45**, 92-98.
17. Y. Kuroda, Y. Miyamoto, M. Hibino, K. Yamaguchi and N. Mizuno, *Chem. Mater.*, 2013, **25**, 2291-2296.
18. N. Chen and R. T. Yang, *J. Catal.*, 1995, **157**, 76-86.
19. F. Cavani, F. Trifirò and A. Vaccari, *Catal. Today*, 1991, **11**, 173-301.
20. S. K. Yun and T. J. Pinnavaia, *Inorg. Chem.*, 1996, **35**, 6853-6860.
21. J. T. Kloprogge and R. L. Frost, *J. Solid State Chem.*, 1999, **146**, 506-515.
22. Z. P. Xu and H. C. Zeng, *Chem. Mater.*, 2001, **13**, 4555-4563.
23. S. Doniach and M. Sunjic, *J. Phy. C: Solid State Phys.*, 1970, **3**, 285.
24. L. Salvati, L. E. Makovsky, J. M. Stencel, F. R. Brown and D. M. Hercules, *J. Phys. Chem.*, 1981, **85**, 3700-3707.
25. B. J. Aronson, C. F. Blanford and A. Stein, *Chem. Mater.*, 1997, **9**, 2842-2851.
26. S. Brunauer, P. H. Emmett and E. Teller, *J. Am. Chem. Soc.*, 1938, **60**, 309-319.
27. C. Komintarachat and W. Trakarnpruk, *Ind. Eng. Chem. Res.*, 2006, **45**, 1853-1856.
28. C. Li, Z. Jiang, J. Gao, Y. Yang, S. Wang, F. Tian, F. Sun, X. Sun, P. Ying and C. Han, *Chem. Eur. J.*, 2004, **10**, 2277-2280.
29. W. Trakarnpruk and K. Rujiraworawut, *Fuel Process. Technol.*, 2009, **90**, 411-414.
30. R. Wang, G. Zhang and H. Zhao, *Catal. Today*, 2010, **149**, 117-121.
31. L. Yang, J. Li, X. Yuan, J. Shen and Y. Qi, *J. Mol. Catal. A: Chem.*, 2007, **262**, 114-118.
32. W. Zhu, W. Huang, H. Li, M. Zhang, W. Jiang, G. Chen and C. Han, *Fuel Process. Technol.*, 2011, **92**, 1842-1848.
33. V. Hulea, A.-L. Maciuca, F. Fajula and E. Dumitriu, *Appl. Catal. A: Gen.*, 2006, **313**, 200-207.
34. A.-L. Maciuca, C.-E. Ciocan, E. Dumitriu, F. Fajula and V. Hulea, *Catal. Today*, 2008, **138**, 33-37.

Table of contents: The $Na_3[PW_{12}O_{40}]$ intercalated tris(hydroxymethyl)aminomethane (Tris)-modified LDHs has been prepared for the first time without necessity of degassing CO_2, resulting in the formation of new intercalated assembly of Tris-LDH-PW_{12} under mild conditions.

Title: Tris(hydroxymethyl)aminomethane Modified Layered Double Hydroxides Largely Facilitate Polyoxometalate Intercalation

Authors: Yang Chen, Dongpeng Yan, and Yu-Fei Song*

TOC figure: